https://doi.org/10.5194/egusphere-2025-4550
Preprint. Discussion started: 15 January 2026

Stable Stream Temperature Prediction for Different Basins Using Time Series Encoding and Temporal Convolutional Networks

Lichen Su[1], Wei Zhao[2]

[1]The School of Environment, Education and Development, University of Manchester, Manchester, UK

[2]Department of Architecture, College of Architecture and Environment, Sichuan University, China

Correspondence to: Lichen Su (lichen.su@postgrad.manchester.ac.uk)

Abstract. Stream temperature prediction is crucial for assessing the health of river ecosystems. In the task of predicting river water temperatures across different river basins (particularly across distinct climatic zones), water temperature datasets are often inconsistently supplied. Concurrently, the spatial heterogeneity within different river basins significantly complicates water temperature forecasting, making it challenging to establish a water temperature prediction model that exhibits strong generalization capabilities and stable predictive outcomes. To address this issue, moving average encoding and DOY encoding of time series data into the temporal convolutional network model are incorporated, thereby constructing a temporal convolutional network model for time series data encoding (TimENC-TCN). This model effectively captures the multimodal characteristics of complex random time series dynamic water temperature data, subsequently yielding stable prediction results across different river basins. Thirteen hydrological stations across four inter-basin rivers (Thames, Colorado, Mississippi, and Sacramento) are used to test the proposed improved TimENC-TCN model and compare its performance with that of reference models (Air2stream, NARX, GRU, and GBOOST). The results indicate that the enhanced features perform well in rivers with minimal human intervention, and that air temperature and DOY are important variables influencing water temperature prediction. The proposed improved model demonstrates more stable and accurate prediction performance in cross-basin water temperature prediction tasks (with an average RMSE on the test set at least 8.7% better than the comparison models). Considering the features and model performance, the proposed model should be a promising approach for stream temperature reconstruction in data-scarce regions across diverse river basins.

1 Introduction

Stream temperature is a key factor influencing the quality of aquatic ecosystems. Stream temperature directly affects the concentration of important substances in rivers as well as the growth and distribution of organisms (Haase, et al., 2023; Zhi, et al., 2023a; Zhi, et al., 2023b). Additionally, stream temperature has a significant impact on urban economies, such as fisheries, thermal power generation, and the entertainment industry (Bonacina, et al., 2023; Noyes and Lema, 2015). Currently, the long-term rise in stream temperature and short-term fluctuations are being observed more frequently (Briciu, et al., 2023; Knez, et al., 2022), and human activities may be a potential factor contributing to these phenomena (Fang, et al.,

https://doi.org/10.5194/egusphere-2025-4550
Preprint. Discussion started: 15 January 2026

2021; Ficklin, et al., 2023). To assess river environmental quality and the impacts of human behaviour, accurate and sufficient stream temperature data are required.

To reconstruct or predict water temperature, process-based models and data-driven models have often been developed in past researches. Process-based models typically require multiple environmental variables as inputs (Michel, et al., 2022), which limits their application across different geographical scales. Improved models such as Air2stream further control computational complexity to seek broader application, yet they remain based on process-based models. Recently, some deep learning models have been shown to have advantages over traditional physical models in stream temperature prediction tasks (Qiu, et al., 2021; Sun, et al., 2024). These models typically require fewer types of variables and demonstrate better accuracy and stability. Among them, air temperature and *DOY* are two common variables (Almeida and Coelho, 2023; Zhu and Piotrowski, 2020). The former is generally considered an important predictive factor and is widely used. The latter is easily obtainable and can serve as an alternative to some hard-to-obtain variables, thereby influencing model performance.

However, current prediction models (including machine learning and deep learning models) do not perform consistently when dealing with spatial heterogeneity. This results in insufficient predictive stability for the same model across different river basins. Piotrowski et al. (2021) found that the four models exhibited significant differences in their predicted stream temperatures across five basins. And multi-layer perceptron neural network (MLP) model showed the lowest and highest mean squared errors of 0.403°C and 3.109°C, respectively. The Air2stream model also demonstrated varying performance in stream temperature predictions across different basins (Callahan and Moore, 2025; Piotrowski and Napiorkowski, 2018; Zhu et al., 2024), and this phenomenon is widespread. These findings highlight the importance of developing a model that can reliably address spatial heterogeneity. Additionally, many hydrological stations lack long-term stream temperature observation data or have gaps in existing observation data. Therefore, the stability performance of the predictive model requires further validation (Almeida and Coelho, 2023).

Given the challenges posed by spatial heterogeneity and low data availability to model performance, stream temperature prediction models need to extract as much information as possible from limited datasets. Compared to the process-based models, it is also noted that end-to-end (Data2data) learning models contribute to addressing spatial heterogeneity. Moreover, making full use of historical time-series data can effectively mitigate the limitations posed by low data availability in water temperature forecasting. Therefore, in model construction, deep learning network based on time series data can be considered for incorporation. This approach can effectively capture the multimodal characteristics of complex random time series dynamic water temperature data, thereby yielding stable prediction results across different river basins. Compared to traditional models, temporal convolutional network (TCN) possesses significant advantages in terms of long-range dependency modelling capabilities, stability, and flexible receptive fields. Therefore, TCN has great development potential in stream temperature data prediction tasks. In terms of feature extraction and selection, to improve the model's prediction accuracy, generalization ability, and training efficiency, the multi-input-output time series encoding (including DOY encoding and time moving average encoding) for deep learning models should be incorporated. In time series data prediction

https://doi.org/10.5194/egusphere-2025-4550
Preprint. Discussion started: 15 January 2026

tasks, these features are easily obtainable and validated, which helps strengthen the model's ability to capture temporal changes.

This study addresses challenges such as insufficient water temperature data availability and spatial heterogeneity interference in river water temperature forecasting across diverse river basins. By integrating moving average coding of time series data, DOY coding, and TCN model, it constructs a stable water temperature TimENC-TCN prediction model suitable for various river basins, particularly across different climatic zones. The results show that the model can handle water temperature prediction across river basins using historical temperature data and improved *DOY* encoding features, and it performs well in mitigating spatial heterogeneity. Even in low-data-availability environments, the TimENC-TCN model demonstrates high predictive stability and accuracy. Therefore, the TimENC-TCN model is beneficial for reconstructing water temperature data across river basins (including those with missing observational data) and provides a reference for water temperature model selection and feature selection.

2 Model calibration and validation data

2.1 Research Area and Dataset

To evaluate the performance of the TimENC-TCN model and other benchmark models (Air2stream, NARX, GBOOST, GRU), 13 hydrological stations on four rivers (Thames, Colorado, Mississippi, and Sacramento) were selected as sources of stream temperature data (Table 1). The four rivers exhibit distinct basin characteristics, and the 13 stations are located in diverse geographical contexts, facilitating the assessment of spatial heterogeneity (Latitude: from 30°26'44.4" to 51°32′26.0916″, Longitude: from -121°49′25″0° to 15′2.4552″). Moreover, the total data volume (ranging from 2100 to 11277) at each water temperature station varies considerably, enabling an assessment of the model's performance under different data volumes and in the presence of missing data. Additionally, air temperature data and DOY data were extracted from nearby meteorological stations. If meteorological stations were unable to provide data, air temperature data were sourced from the NASA Power Project. During calibration, the dataset was divided into training, validation, and test sets in an 8:1:1 ratio based on temporal order.

Table 1: River hydrological station information

No	River	Station	station number	Latitude	Longitude	Measurement Period	Total data volume
1	Colorado	Cameo	a (09095500)	39°14'21"	-108°15'56"	1994/1/1 - 2025/6/29	11277
2	Colorado	Catamount bridge	b (09060799)	39°53'27.96"	-106°49'54.10"	2016/10/21 - 2025/6/29	6822
3	Colorado	Cisco	c (09180500)	38°48'38"	-109°17'34"	2006/8/26 - 2025/6/29	2100
4	Colorado	Glenwood springs	d (09071750)	39°33'32"	-107°17'25"	1995/10/1 - 2025/6/29	10707
5	Colorado	Yuma	e (09522005)	32°42'44"	-114°43'20"	2017/1/23 - 2025/6/29	3057
6	Mississippi	Baton Rouge	f (07374000)	30°26'44.4"	-91°11'29.6"	2004/10/1 - 2025/2/9	6761

https://doi.org/10.5194/egusphere-2025-4550
Preprint. Discussion started: 15 January 2026

7	Mississippi	Cape Girardeau	g (07020850)	37°18'06.8"	-89°31'04.8"	2014/3/14 - 2025/6/5	3694
8	Sacramento	Freeport	h (11447650)	38°27'20.39"	-121°30'05.82"	1998/4/13 - 2023/3/20	6045
9	Sacramento	Verona	i (11425500)	38°46'28"	-121°35'50"	2008/2/13 - 2017/6/30	3361
10	Sacramento	Wilkins Slough	j (11390500)	39°00'36"	-121°49'25"	1981/1/1 - 2011/12/31	10867
11	Thames	Brentford Barge	k (BREPON)	51°28′47.3196″	-0°18′11.1744″	2009/1/1 - 2024/12/31	5045
12	Thames	Purfleet	l (E03036A)	51°28′13.368″	0°15′2.4552″	2009/1/8 - 2024/12/31	5718
13	Thames	Taplow	m (M01023A)	51°32′26.0916″	-0°41′40.6068″	2018/1/1 - 2024/12/31	2450

2.2 Verification Data and Variables Introduction

When predicting daily water temperature, daily air temperature (T_{air}), 7-day moving average air temperature ($\overline{T}_{air}$), and *DOY* encoding are used as input variables, with the output variables being daily stream temperature (T_{stream}) and 7-day moving average stream temperature ($\overline{T}_{stream}$). In the model, the 7-day moving average air temperature/stream temperature is used to smooth out abnormal data and enhance the capture of temporal features. The *DOY* feature is included to capture the temporal variation characteristics of air temperature and water temperature. To further enhance this feature, *DOY* is encoded using cosine/sine functions encoding. Cosine/sine functions encoding maps each location to a unique vector using a series of sine and cosine functions of different frequencies. The encoding for different locations is distinct and changes smoothly with location. Relative spatial relationships can be reflected through the dot product or distance between codes. This encoding possesses a certain linear relationship, facilitating the model to learn its displacement invariance law.

3 Method

The algorithm flowchart for this study is shown in Figure 1. After obtaining the raw data and performing preprocessing such as data denoising, the air temperature, stream temperature, and corresponding date data are extracted. Then, the date data encoding is converted to *DOY* and *DOY* encoding. Subsequently, a 4-layer TCN model and a comparison model are used to predict the water temperature and evaluate the model performance. In addition, to assess performances of *DOY* and *DOY* encoding etc., ablation experiments are conducted. Finally, the robustness of the model under varying data availability was further evaluated through robustness experiments involving the gradual removal of samples.

https://doi.org/10.5194/egusphere-2025-4550
Preprint. Discussion started: 15 January 2026

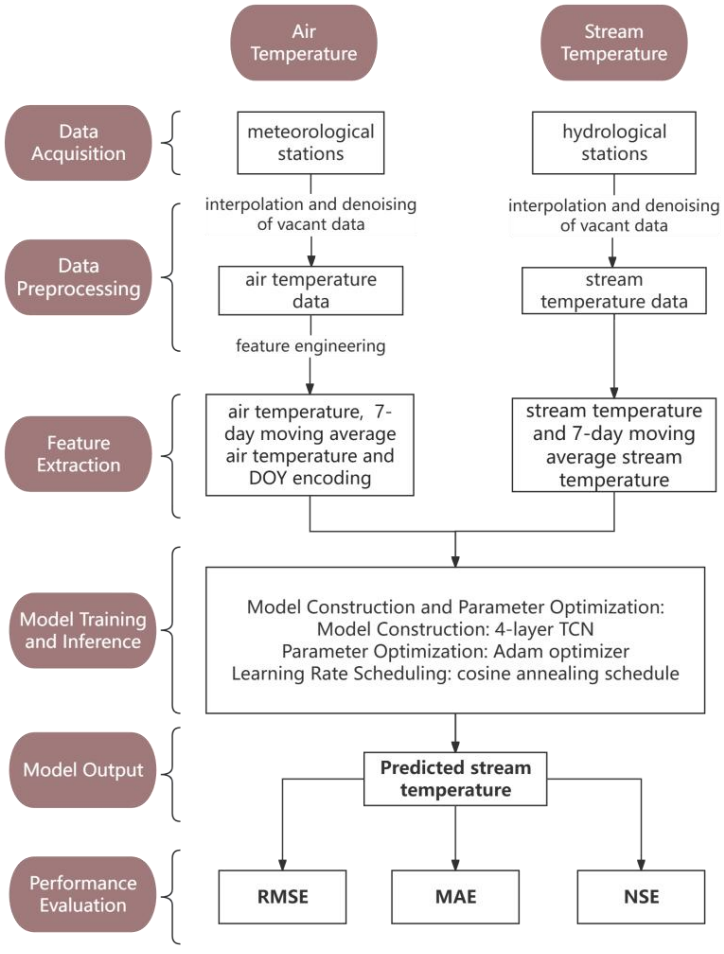

Figure 1: The algorithm flowchart of TimENC-TCN model.

3.1 Features selection and extraction

In feature engineering, to optimize model performance, reduce redundancy, and improve interpretability, the correlation between air temperature, *DOY*, and stream temperature needs to be tested. As shown in Figure 2 and Table 2, there is a strong linear relationship between the input variable air temperature and the output variable water temperature (Fig.1), and the Pearson correlation coefficient $\rho_{X,Y}$ (Eq.1) adequately reflects the strength of the association (Table 2). In contrast, the relationship between the input feature *DOY* and the output variable stream temperature exhibits strong non-linear characteristics (Fig.2), and the Pearson correlation coefficient may underestimate the true dependency relationship. In such cases, the distance correlation coefficient *dCor* (Eq.2) provides a more reliable measure of association (Table 2). Correlation analysis indicates that air temperature has significant predictive power through a linear dependency relationship, while the

https://doi.org/10.5194/egusphere-2025-4550
Preprint. Discussion started: 15 January 2026

seasonal or periodic patterns reflected by *DOY* are better captured using non-linear indicators. Therefore, combining linear and non-linear features is crucial for more accurate river temperature prediction.

$$\rho_{X,Y} = \frac{Cov(X,Y)}{\sigma_x \sigma_y}, \tag{1}$$

$$dCor(X,Y) = \frac{dCov(X,Y)}{\sqrt{dVar(X)}\sqrt{dVar(Y)}}, \tag{2}$$

Where X, Y are input variables, $Cov(X,Y)$ is the covariance of variables X and and Y, σ_* is the standard deviation of the variables, $dCov(X,Y)$ is the distance covariance of the variables, and $dVar(X,Y)$ is the distance variance of the corresponding variables.

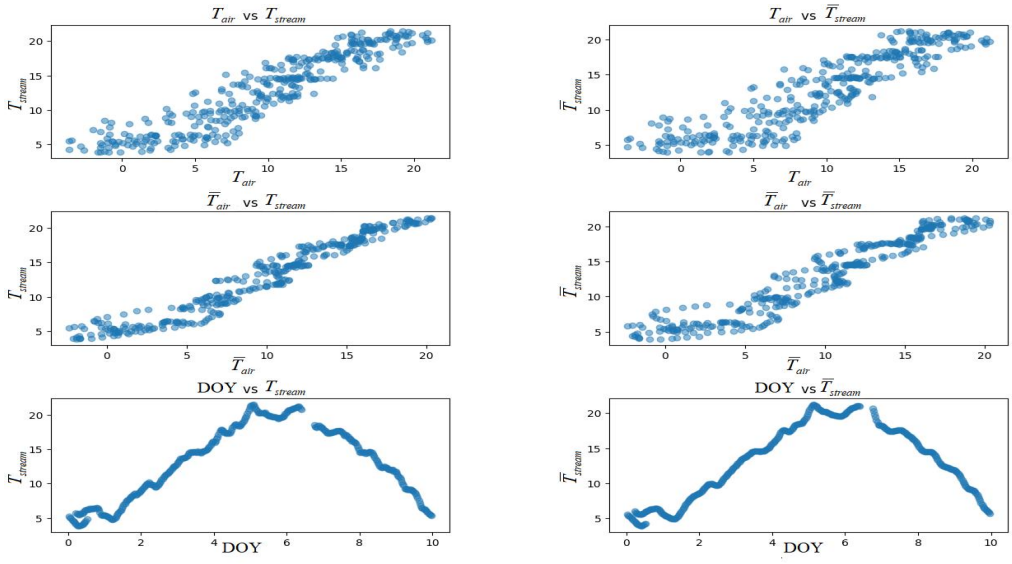

Figure 2: Feature correlation diagram.

Table 2: Feature Pearson coefficients and distance correlations. (Note: ρ above 0.7 are considered to indicate strong linear correlation. $dCor$ values above 0.6 are interpreted as moderate nonlinear dependencies.)

Input feature / Output feature	T_{air}	$\overline{T}_{air}$	DOY
T_{stream}	$\rho = 0.931$	$\rho = 0.971$	$dCor = 0.626$
$\overline{T}_{stream}$	$\rho = 0.910$	$\rho = 0.958$	$dCor = 0.649$

To further enhance the model's expressive and generalization capabilities, it is necessary to further enhance the feature temperature and *DOY*. Considering the noise and short-term fluctuations in temperature data, which affect the model's ability

https://doi.org/10.5194/egusphere-2025-4550
Preprint. Discussion started: 15 January 2026

to capture the air-stream temperatures relationship, a 7-day moving average temperature is introduced to smooth the data and remove noise. Then, considering that when DOY is directly input into the model as a numerical sequence, the periodic characteristics of the data may not be fully expressed. Using trigonometric functions to represent the periodicity of *DOY* (Eq.3 and Eq.4) helps preserve periodic features, avoid the misleading effects of linear assumptions, and improve the model's predictive performance. In summary, the input features are set as daily air temperature (T_{air}), 7-day moving average air temperature ($\overline{T}_{air}$), and the encoded form of DOY (sin_DOY, cos_DOY).

$$sin\_DOY = sin(\frac{2\pi \times DOY}{D}) , \quad (3)$$

$$cos\_DOY = cos(\frac{2\pi \times DOY}{D}), \quad (4)$$

Where D is the number of days in a year.

3.2 Model construction

Deep learning networks can extract complex features from large amounts of raw data and learn to make predictions. This makes deep learning networks a powerful tool for prediction, optimization, and understanding in the increasingly complex and data-rich environment of stream temperature prediction. Through literature research, Air2stream, NARX, GBOOOST and GRU were found to be widely used in stream temperature prediction and were therefore selected as comparison models.

3.2.1 TimENC-TCN model

TimENC-TCN is a convolution-based sequence modelling method for handling time series data, which uses temporal convolution operations instead of ordinary convolution for sequence modelling. Its core pipeline is to construct a deep network by stacking multiple TimENC-TCN Blocks to model the long-term dependencies of time series data, and finally output the final results through a fully connected layer. The network includes causal convolution, dilated convolution, and residual connections. It can ensure that each time step in the TimENC-TCN input does not depend on future inputs but only on the current time step t and its preceding inputs, thereby preserving temporal causality. Additionally, to expand the receptive field without increasing parameter input, holes are introduced into the convolution kernels; Finally, to address the challenges of training deep neural networks and the vanishing gradient problem, residual connections are incorporated into the network structure.

The TimENC-TCN Block (Fig. 3) is the basic unit that constitutes the entire model. Its core objective is to extract multi-scale features from sequences while maintaining temporal causality, ensuring the stability and effectiveness of deep network training. As shown in Figure 3, the Block includes Conv1d, BatchNorm1d, ReLU, Dropout, and Residual Connection. Among these, Conv1d is used to extract temporal features and learn relationships between adjacent time steps. BatchNorm1d standardizes all channels, mitigating gradient explosion issues and reducing dependence on initialization. ReLU is used to

https://doi.org/10.5194/egusphere-2025-4550
Preprint. Discussion started: 15 January 2026

introduce non-linear expression relationships. Dropout enhances the model's generalization ability and prevents overfitting. Finally, the Residual Connection addresses the challenges of training deep networks, such as gradient vanishing and decay.

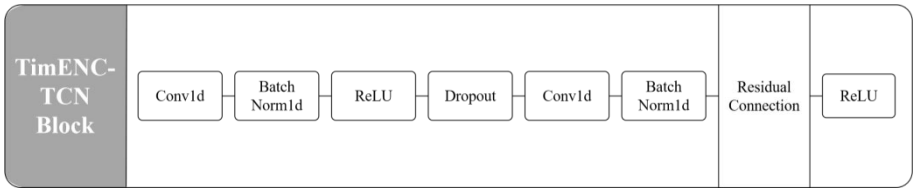

Figure 3: TimENC-TCN block.

The TimENC-TCN network used in this study consists of four convolutional layers (Fig. 4), with zero-padding used to maintain the length of the time series. Each convolutional layer sequentially extracts features at different time scales, with the final output used to predict the target variable. TimENC-TCN captures dependencies across multiple time scales through inter-layer residual structures and dilated causal convolutions, without relying on recursive mechanisms, thereby avoiding gradient issues during training with long sequences. In the architecture, 1D causal convolutions ensure that the output depends only on the current and past time steps. In dilated convolutions, the receptive field grows exponentially with the layer number, with a dilation factor of 2^d (where d is the d^{th} layer), effectively capturing long-range dependencies. To address the vanishing gradient problem, a residual module is used, which includes two layers of dilated causal convolutions (ReLU and dropout) and residual skip connections. In this model, the input sequence length for the TimENC-TCN is set to 7, meaning the model uses the past 7-time steps for each prediction.

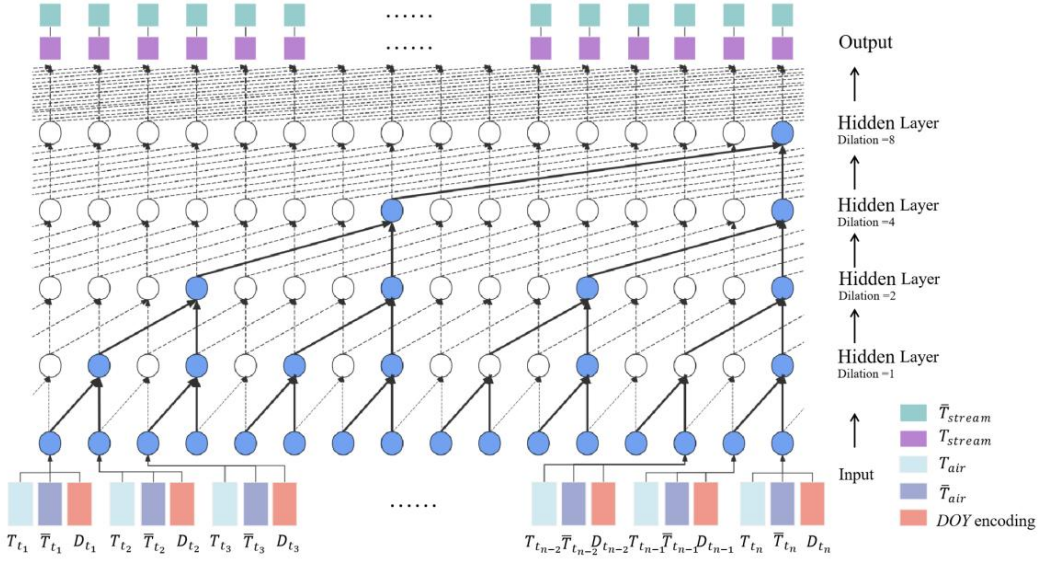

Figure 4: TimENC-TCN framework.

https://doi.org/10.5194/egusphere-2025-4550
Preprint. Discussion started: 15 January 2026

To enhance the stability and generalization capability of model training, this study employed multiple optimization strategies during the training process of the TimENC-TCN model. First, the Adam optimizer was selected. Its adaptive learning rate mechanism effectively accelerates the convergence process, and by setting a larger parameter beta=0.98, it reinforces the smooth estimation of the second-order momentum of the gradient. Additionally, weight decay (weight decay=0.01) was introduced to control model complexity and prevent overfitting. Second, the cosine annealing learning rate scheduler was adopted to dynamically adjust the learning rate during training. This strategy gradually reduces the learning rate within training epochs and ultimately converges to the minimum learning rate, thereby maintaining the model's fine-grained optimisation capability in the later training stages. Additionally, the training loss and validation loss for each round are tracked during training to monitor model performance and assist in subsequent parameter tuning.

3.2.2 Air2stream model

The Air2stream model is a modified version of the Taylor series expansion based on the concentrated heat balance exchange in rivers (Eq. 5). In this model, water temperature and flow rate are used as inputs, and heat exchange between rivers, tributaries, and the atmosphere is considered, with the final output being stream temperature. The basic air2stream model has eight parameters (Eq. 6), which are expressed as follows:

$$c_p V \frac{dT_{stream}}{dt} = AH + \rho c_p \left(\sum_i Q_i T_{w,i} - Q T_w \right), \tag{5}$$

$$c \frac{dT_{stream}}{dt} = \frac{1}{\theta^{a_4}} \left(a_1 + a_2 T_{air} - a_3 T_{stream} + a_6 cos\left(2\pi \left(\frac{t}{t_y} - a_7\right)\right) - a_8 T_{stream} \right), \tag{6}$$

Where t represents time, ρ represents the density of the water body, c_p represents the specific heat capacity at constant pressure, A represents the surface area of the river segment, H represents the net heat flux at the river-atmosphere interface, Q represents the flow rate of the downstream river segment, Q_i and $T_{w,i}$ represent the flow rate and temperature of the i^{th} contributing water flux (tributary, possibly including groundwater), respectively, V represents the total volume responding to the heat flux. θ is the dimensionless flow rate, t_y is the time over an entire year, and $a_1 - a_8$ are model parameters.

By adjusting the pulsatile flow parameter settings, the Air2stream model can be controlled to use only temperature time series as input, which is useful for evaluating the model's performance under the same input parameters. Ignoring the effect of pulsatile flow yields a 5-parameter model version (Eq. 7).

$$\frac{dT_{stream}}{dt} = a_1 + a_2 T_{air} - a_3 T_{stream} + a_6 cos\left(2\pi \left(\frac{t}{t_y} - a_7\right)\right), \tag{7}$$

Furthermore, assuming that the flow rate is constant, Air2stream can be further simplified to a 3-parameter version (Eq. 8).

$$\frac{dT_{stream}}{dt} = a_1 + a_2 T_{air} - a_3 T_{stream}, \tag{8}$$

In this study, since the effect of flow on water temperature was not considered, two models (Eq. 7- 8) of the 3/5 parameter version were selected for testing on all hydrological station data, and the optimal value was marked as *Air2stream_best*. For

https://doi.org/10.5194/egusphere-2025-4550
Preprint. Discussion started: 15 January 2026

more detailed information, please refer to the work of Toffolon and Piccolroaz (2015) and the link to the model (https://github.com/spiccolroaz/air2stream).

3.2.3 NARX model

NARX is a specific category of recurrent neural networks (RNN), consisting of interconnected nodes inspired by biological neural systems. Each node receives one or more inputs, processes them through a nonlinear function, and produces an output. This model combines the system's own historical outputs (autoregressive) and external input signals (exogenous variables) to predict future outputs. NARX has a strong ability to capture nonlinear relationships and clearly incorporates lagged outputs and external inputs, making it highly interpretable. The basic equation for the NARX network used in time series forecasting can be expressed as in Eq. 9:

$$y(t) = F(y(t-1), y(t-2), \cdots, y(t-n_y), u(t-1), u(t-2), \cdots, u(t-n_u)), \quad (9)$$

Where $y(t)$ is the system output at time t (i.e., the value to be predicted), $u(t)$ is the external input to the system at time t, n_y is the order of the output delay (the maximum lag number used for historical outputs), n_u is the order of the input delay (the maximum lag number used for historical inputs), and $F(*)$ is a nonlinear function.

3.2.4 GBOOST model

GBOOST is a powerful ensemble learning algorithm. It starts with a set of simple models and, at each step, models the error of the previous model (the 'gradient' direction), ultimately combining the results of multiple weak learners through weighted summation. It is suitable for various structured data and can capture non-linear relationships and handle missing values and categorical variables. GBOOST often demonstrates high accuracy and strong generalisation capabilities. A standard GBOOST model can be represented as in Eq. 10:

$$\hat{y}(t) = \sum_m^M r_m h_m(x), \quad (10)$$

Where $\hat{y}(t)$ refers to the model's final prediction for input x, M is the total number of weak learners, $h_m(x)$ refers to the m^{th} weak learner (usually a regression tree), and r_m is the learning rate or step size for the m^{th} round (which can be a fixed constant or calculated through row minimisation).

3.2.5 GRU model

As a variant of recurrent neural networks (RNN), gated recurrent units (GRU) introduce update gates and reset gates to control the retention and forgetting of information, effectively alleviating the vanishing gradient problem faced by traditional RNN when processing long sequences. Compared with long short-term memory networks (LSTM), GRUs have the advantages of lightweight structure and fast training convergence speed. A standard GRU model can be represented as follows:

$$z_t = \sigma(W_z x_t + U_z h_{t-1} + b_z), \quad (11)$$

https://doi.org/10.5194/egusphere-2025-4550
Preprint. Discussion started: 15 January 2026

$$z_t = \sigma(W_z x_t + U_z h_{t-1} + b_z), \quad (12)$$

$$\tilde{h}_t = \tanh(W_h x_t + U_h(r_t \odot h_{t-1} + b_h), \quad (13)$$

$$h_t = (1 - z_t) \odot \tilde{h}_{t-1} + z_t \odot \tilde{h}_{t-1}, \quad (14)$$

Where x_t is the input vector at time step t, h_t is the hidden state at time step t (i.e., the output of the GRU), h_{t-1} is the hidden state at the previous time step, z_t is the update gate vector (determining how much old information to retain), and r_t is the reset gate vector (determining how much of the old state to forget). $\tilde{h}_t$ is the candidate hidden state (new memory), and $W_*/U_*/b_*$ are learnable parameters (weight matrices and biases).

3.3 Model Performance Comparison

To evaluate the performance of the model, three widely used metrics, RMSE, MAE and NSE (Eq. 15-Eq. 17) were used.

$$RMSE = \sqrt{\frac{1}{n}\sum_{i=1}^{n}(T_M^i - T_M^o)^2}, \quad (15)$$

$$MAE = \frac{1}{n}\sum_{i=1}^{n}\left|T_M^i - T_M^o\right|, \quad (16)$$

$$NSE = 1 - \frac{\frac{1}{n}\sum_{i=1}^{n}(T_M^i - T_M^o)^2}{\frac{1}{n}\sum_{i=1}^{n}(T_M^i - \overline{T}_M^o)^2}, \quad (17)$$

Where T_M^i and T_M^o are the model and observation data of the water temperature of the i^{th} river, $\overline{T}_M^o$ is the average value of T_M^o, and n is the number of samples.

4 Results

4.1 Feature-related results

To identify the optimal feature inputs for model prediction performance, ablation experiments were conducted on all rivers using the TimENC-TCN model. During water temperature prediction, ablation experiments were conducted on the input features to further analyse the contribution of air temperature, *DOY*, and *DOY* time series to model performance. The ablation experiments were divided into three groups.

Option	Feature input	Feature output
#1	T_{air}	T_{stream}
#2	T_{air}, DOY	T_{stream}
#3	$T_{air}, \overline{T}_{air}, DOY$	$T_{stream}, \overline{T}_{stream}, DOY$

The results in Table 3 indicate that Option 3 (#3) generally improves model performance compared to Option 1 (#1) and 2 (#2) with the average RMSE improving by up to 4.7%. Among the three options, Option 1's model prediction performance was significantly worse (average RMSE: training set 1.447°C, validation set 1.583°C, test set 1.55°C) than Option 2, which incorporates *DOY* (average RMSE: training set 0.974°C, validation set 1.144°C, test set 1.118°C) and Option 3 (average RMSE: training set 0.94°C, validation set 1.095°C, test set 1.066°C). This indicates that *DOY* is an important factor

https://doi.org/10.5194/egusphere-2025-4550
Preprint. Discussion started: 15 January 2026

influencing the performance of water temperature prediction models. It is noted that at the Baton Rouge, Cape and Purfleet stations (station f, g and l), Option 3 (average RMSE of the test set across the three stations: 1.159°C) showed a significant improvement in TimENC-TCN prediction performance compared to Option 2 (average RMSE of the test set across the three stations: 1.17°C). As described in Sect. 3.1, the enhanced features used in Option 3 (7-day moving average temperature, *DOY* cosine encoding) strengthen the model's ability to capture the temporal variation characteristics of water temperature. Therefore, the results of Option 3 indicate that capturing temporal variation relationships is crucial in water temperature prediction tasks, especially at stations where temporal variations are not fully captured. It is also worth noting that at stations Yuma, Verona and Wilkins (station e, i and j), the model performance of Option 3 is slightly lower than that of Option 2. At the Verona station (station i), the performance decline is most pronounced. This station is located on the Sacramento River, which is managed for water allocation by the Central Valley Project. The temperature at this station is influenced by human factors. Therefore, it is reasonable to infer that at these stations where performance has declined, human factors have masked the effects of natural factors, thereby weakening the direct explanatory power of temperature, *DOY*, or *DOY* encoding.

Table 3: RMSE results of the ablation experiments.

Station	Option 1			Option 2			Option 3		
	Trainng	Validation	Test	Training	Validation	Test	Training	Validation	Test
a	1.685	1.85	1.808	1.063	1.336	1.069	1.045	1.333	**1.04**
b	1.306	1.423	1.268	1.005	1.23	1.225	0.962	1.12	**1.189**
c	1.675	1.863	1.781	1.202	1.296	1.136	1.165	1.289	**1.065**
d	1.504	1.575	1.569	0.923	1.08	0.868	0.903	1.075	**0.845**
e	1.021	1.128	1.111	0.699	0.905	**0.675**	0.677	0.876	0.679
f	2.715	3.103	2.775	1.243	1.178	1.246	1.127	1.068	**1.137**
g	1.781	1.963	1.627	1.08	1.423	1.111	0.989	1.313	**0.987**
h	1.3	1.666	1.396	1.172	1.447	1.319	1.163	1.419	**1.29**
i	1.451	1.008	1.723	1.104	1.222	**1.835**	1.066	1.225	1.862
j	1.265	1.128	1.297	1.032	0.904	**0.967**	1.03	0.904	0.969
k	1.139	1.074	1.113	0.875	0.903	0.812	0.879	0.84	**0.786**
l	1.201	1.201	1.143	0.701	0.64	0.79	0.589	0.468	**0.543**
m	0.943	1.044	0.938	0.515	0.668	0.691	0.541	0.626	**0.641**

4.2 Model-related results

In 100 repeated experiments across all tested stations, the proposed TimENC-TCN model demonstrated superior predictive accuracy and stability compared to other models. The RMSE values for the TimENC-TCN validation set (Table 4) ranged from 0.468°C to 1.419°C (average: 1.043°C), the MAE values (Fig. 5) ranged from 0.5°C to 1.1°C (average: 0.872°C), and all NSE values (Fig. 5) exceeded 0.93 (range: 0.931–0.991, average: 0.963). Except for the Catamount Bridge, Cape, and Verona stations, the TimENC-TCN demonstrated the best predictive performance across all models. In the test set, the

https://doi.org/10.5194/egusphere-2025-4550
Preprint. Discussion started: 15 January 2026

RMSE of the TimENC-TCN model ranged from 0.543 °C to 1.862 °C (average: 1.003 °C), the MAE fluctuated between 0.527°C and 1.408°C (average: 0.865°C), and the NSE (excluding Verona) 0.925 and 0.989 (average: 0.968). The TimENC-TCN model achieved the best prediction results at 12 out of 13 test stations. Notably, overfitting was evident at the Verona station on the Sacramento River (Table 4). As described in Sect. 4.1, this indicates that the TimENC-TCN model using *DOY* and air temperature as inputs has a better ability to handle spatial heterogeneity in basins influenced by natural environmental factors, while stations influenced by human factors require additional feature learning.

Table 4: RMSE of validation sets and test sets for each model.

Station	Air2stream (*Air2stream_best*)	NARX	GBOOST		GRU		TimENC-TCN	
	Test	Test	Validation	Test	Validation	Test	Validation	Test
a	1.937	1.954	*1.437*	1.121	*1.514*	1.174	***1.333***	**1.04**
b	1.547	1.923	*1.17*	1.266	*1.147*	1.319	***1.12***	**1.189**
c	1.761	2.217	*1.413*	1.164	*1.343*	1.309	***1.289***	**1.065**
d	1.703	2.066	*1.188*	0.913	*1.293*	1.027	***1.075***	**0.845**
e	1.198	1.663	*0.934*	0.782	*1.334*	1.059	***0.876***	**0.679**
f	1.349	1.561	*1.227*	1.314	*1.244*	1.217	***1.068***	**1.137**
g	**0.888**	1.729	*1.515*	1.192	*1.558*	1.211	***1.313***	0.987
h	1.655	2.229	*1.444*	1.361	*1.702*	1.505	***1.419***	**1.29**
i	**1.477**	2.5	*1.279*	1.915	***1.163***	1.646	*1.225*	1.862
j	1.315	1.676	*0.921*	1.003	*0.979*	1.068	***0.904***	**0.969**
k	1.085	1.766	*0.881*	0.832	*1.168*	0.903	***0.84***	**0.786**
l	0.742	1.246	*0.675*	0.761	*0.644*	0.705	***0.468***	**0.543**
m	0.903	1.112	*0.73*	0.786	*0.843*	0.834	***0.626***	**0.641**

Box plots (Fig. 5) further illustrate the variability in the performance of different water temperature prediction models across various geographical contexts. Among these, the NARX model exhibits significant variability in prediction performance across different stations (RMSE: 1.112°C–2.5°C, MAE: 0.8°C–2.056°C, NSE: 0.638–0.965), indicating its inability to effectively address water temperature prediction tasks under diverse geographical conditions. Although the Air2stream model has a lower RMSE in some cases, its box size is large, indicating significant performance variability and poor performance at certain stations. Among models with smaller box sizes (GBOOST, GRU and TimENC-TCN), TimENC-TCN has the highest average evaluation metrics, meaning its results not only exhibit low variability and high-performance stability but also achieve the best overall performance.

https://doi.org/10.5194/egusphere-2025-4550
Preprint. Discussion started: 15 January 2026

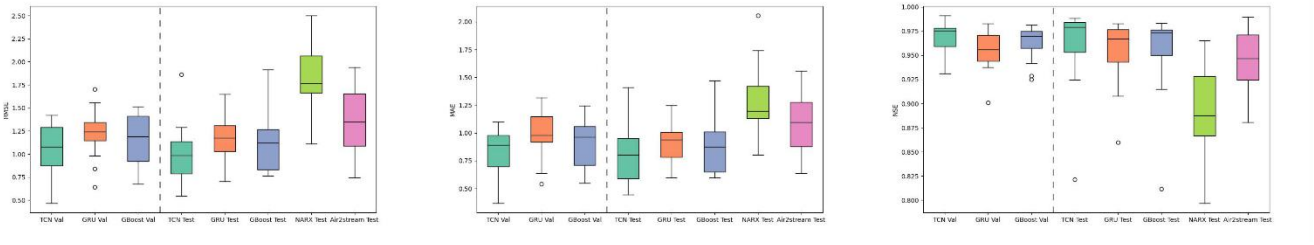

Figure 5: Performances of different models in validation and test sets (a) RMSE (b) MAE (c) NSE.

Without losing generality, the Purfleet station (Station l) is taken as an example. Figure 6 shows the predicted and observed water temperatures in the Purfleet station. As shown in the figure 6, although the TimENC-TCN model exhibited some fluctuations during the training phase, the overall absolute error remained stable and at a low level (average absolute error: training set 0.406°C, validation set 0.364°C, test set 0.440°C). Figure 7 shows that the predicted water temperature values in the TimENC-TCN model's observed-predicted scatter plot are close to the 1:1 line, further indicating that the TimENC-TCN model has excellent water temperature prediction performance.

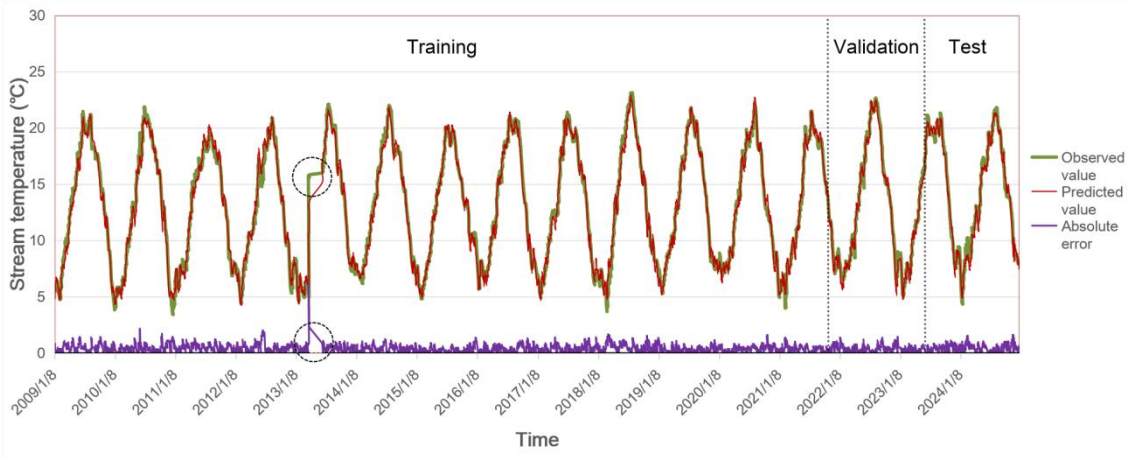

Figure 6: Observation values, prediction values, and absolute Errors at the Purfleet station.

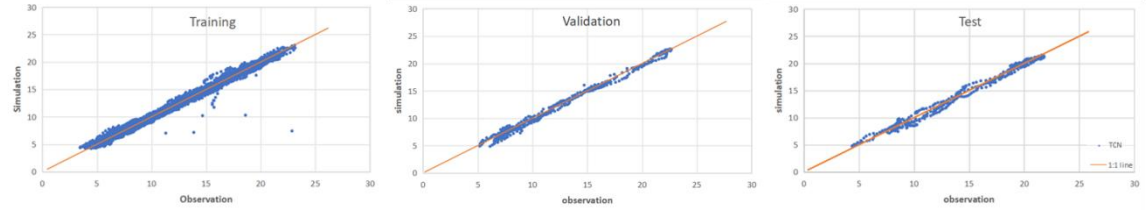

Figure 7: The observation-test scatter plot at the Purfleet station and 1:1 line.

https://doi.org/10.5194/egusphere-2025-4550
Preprint. Discussion started: 15 January 2026

315 To test the generalisation performance of the TimENC-TCN model, a gradual sample removal experiment was conducted. In this experiment, 5% of non-repeated samples were randomly removed from the training set in each round until the training samples were reduced to 40% of the initial dataset. Taking the Purfleet station as an example, the various evaluation metrics of the TimENC-TCN model in each round of the removal experiment are shown in Figure 8.

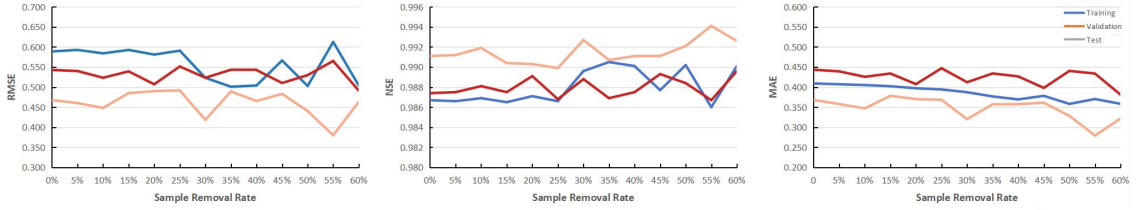

320 **Figure 8: Line chart of RMSE performance analysis with sample removal at Purfleet station**

The experimental results indicate that as the removal rate gradually increases, the predictive performance of the TimENC-TCN model remains stable. In the training, validation, and test sets, the RMSE variation does not exceed ±0.056 °C, the MAE variation does not exceed ±0.033 °C, and 8the NSE variation does not exceed ±0.002. As shown in the line chart 325 (Figure 8), the data remains relatively stable across all change rates, with small fluctuations and no significant upward or downward trends, indicating that the indicator is in a stable state. This suggests that the model possesses good temporal generalization capability and exhibits low sensitivity to sample structure, demonstrating high robustness and reliability.

5 Discussions and conclusions

5.1 The impact of characteristics on models

330 Under all tested geographical conditions, air temperature and *DOY* are important predictive variables for stream temperature. The results of feature correlation analysis and ablation experiments indicate that the inclusion of *DOY* can improve the model's ability to capture nonlinear relationships in stream temperature predictions. *DOY* can be extracted from stream temperature or air temperature datasets with low difficulty, so it is recommended to apply this feature in more water temperature prediction models to achieve better performance. *DOY*-encoded features and air temperature seven-day average 335 moving features indicate that time series relationships may be important in stream temperature prediction. In ablation experiments, time series-related features were enhanced. Results show that, under general conditions, enhancing the model's capture of time series relationships can improve model performance. Meanwhile, the case of the Verona station and experiments on the drivers of stream temperature changes (Alger et al., 2021; Wade, et al., 2023) indicate that introducing other features is necessary at stations with significant human interference.

https://doi.org/10.5194/egusphere-2025-4550
Preprint. Discussion started: 15 January 2026

5.2 Spatial heterogeneity

The selected hydrological stations exhibit differences in geographical environment and spatial-temporal scales. However, the TimENC-TCN model demonstrates commendable predictive performance across diverse geographical contexts and outperforms other comparison models (Air2stream, NARX, GRU, GBOOST) in terms of stability and accuracy. In stepwise sample removal experiments, the TimENC-TCN model maintains stable predictive performance across all removal rates. This indicates that the TimENC-TCN model does not rely on specific samples and can still achieve good results in small-sample tests. The results also show that in stream temperature prediction tasks, TimENC-TCN does not require complete stream temperature data as input, which is advantageous for TimENC-TCN in handling prediction tasks with different data structures. However, the performance of TimENC-TCN in water temperature prediction tasks at special stations such as dams (Shi, et al., 2021; Soomro, et al., 2023) needs further testing. Additionally, the test data were obtained from hydrological stations in four large and medium-sized river basins, and complex internal hydrological changes exist in rivers of different grades (Jackson et al., 2017; Tomkins et al., 2024). In summary, although TimENC-TCN has demonstrated its potential for stable stream temperature prediction across different geographical contexts, further testing and improvement in more diverse water temperature prediction tasks are necessary.

5.3 Model applications

This study proposes a method combining feature enhancement with the TCN model for stream temperature reconstruction tasks in regions with limited data availability. Under conditions where only air temperature, *DOY*, and enhanced features are available, the TimENC-TCN model can reliably predict water temperature. Platforms such as EURO-CORDEX (Jacob, et al.,2014) provide access to future air temperature time series data, which meet the feature input requirements of the TimENC-TCN method, thereby enabling the prediction of long-term stream temperature changes in the future. TimENC-TCN also demonstrates its performance stability in cross-basin water temperature prediction tasks primarily influenced by natural factors. This makes TimENC-TCN a promising candidate for reconstructing water temperature data or serving as a reference model in numerous data-scarce regions with diverse geographical and climatic conditions, thereby providing foundational data for related research (hydrological forecasting, climate analysis, etc.) and water resource management (Van, et al., 2023), ecological conservation (Zhao, et al., 2023), and health monitoring (Yu, et al., 2023).

5.4 Conclusions

At 13 hydrological stations in four river basins, the TimENC-TCN, Air2stream, NARX, GRU, and GBOOST models were used to reconstruct daily stream temperature data and compare their predictive performance. Subsequently, ablation experiments and stepwise sample removal experiments were conducted to test the optimal feature inputs and model performance under low data availability conditions. The results are as follows:

(1) In rivers primarily influenced by natural factors, incorporating DOY Sine-Cosine encoding and 7-day average

https://doi.org/10.5194/egusphere-2025-4550
Preprint. Discussion started: 15 January 2026

temperature is an effective method to enhance model performance.

(2) TimENC-TCN demonstrates stable and excellent model prediction performance. In general, TimENC-TCN outperforms other models in terms of validation set and test set performance. Therefore, there is reason to test or apply the TimENC-TCN model in more diverse water temperature prediction tasks.

(3) TimENC-TCN's performance under low data availability and cross-basin testing demonstrates its potential to assist in water temperature prediction in regions with inadequate data collection and monitoring infrastructure.

6 Data and model availability

The dataset and code for the TimENC-TCN model are available via Zenodo: https://doi.org/10.5281/zenodo.17185045 (Su, 2025).

Author contributions

LS: Conceptualization, Formal analysis, Investigation. Data curation, Validation, Visualization, Software, Writing – original draft, review & editing

WZ: Resources, Funding acquisition, Project administration, Supervision, Writing – review & editing.

Declaration of Competing Interest

The authors declare that they have no known competing financial interests or personal relationships that could have appeared to influence the work reported in this paper

Acknowledgements

We are grateful for the support from the National Natural Science Foundation of China under Grant 51878558.

References

Almeida, M. C. and Coelho, P. S.: Modeling river water temperature with limiting forcing data: Air2stream v1.0.0, machine learning and multiple regression, Geosci. Model Dev., 16, 4083-4112, https://doi.org/10.5194/gmd-16-4083-2023, 2023

Alger, M., Lane, B. A., and Neilson, B. T.: Combined influences of irrigation diversions and associated subsurface return flows on river temperature in a semi-arid region, Hydrol. Processes, 35, https://doi.org/10.1002/hyp.14283, 2021.

Bonacina, L., Fasano, F., Mezzanotte, V., and Fornaroli, R.: Effects of water temperature on freshwater macroinvertebrates: a systematic review, Biol. Rev., 98, 191-221, https://doi.org/10.1111/brv.12903, 2023.

https://doi.org/10.5194/egusphere-2025-4550
Preprint. Discussion started: 15 January 2026

Briciu, A.-E., Mihăilă, D., Oprea, D. I., and Prisăcariu, A.: Urban Stream Temperature Surge—Streamwater Temperature Variability after Rainfall in Suceava City Metropolitan Area, Sustainability, 15, https://doi.org/10.3390/su15107882, 2023.

Callahan, L. and Moore, R. D.: Evaluation of the Hybrid Air2stream Model for Simulating Daily Stream Temperature During Extreme Summer Heat Wave and Autumn Drought Conditions, Hydrol. Processes, 39, https://doi.org/10.1002/hyp.70033, 2025.

Fang, L., Wang, L., Chen, W., Sun, J., Cao, Q., Wang, S., and Wang, L.: Identifying the impacts of natural and human factors on ecosystem service in the Yangtze and Yellow River Basins, J. Cleaner Prod., 314, https://doi.org/10.1016/j.jclepro.2021.127995, 2021.

Ficklin, D. L., Hannah, D. M., Wanders, N., Dugdale, S. J., England, J., Klaus, J., Kelleher, C., Khamis, K., and Charlton, M. B.: Rethinking river water temperature in a changing, human-dominated world, Nat. Water, 1, 125-128, https://doi.org/10.1038/s44221-023-00027-2, 2023.

Haase, P., Bowler, D. E., Baker, N. J., Bonada, N., Domisch, S., Garcia Marquez, J. R., Heino, J., Hering, D., Jahnig, S. C., Schmidt-Kloiber, A., Stubbington, R., Altermatt, F., Alvarez-Cabria, M., Amatulli, G., Angeler, D. G., Archambaud-Suard, G., Jorrin, I. A., Aspin, T., Azpiroz, I., Banares, I., Ortiz, J. B., Bodin, C. L., Bonacina, L., Bottarin, R., Canedo-Arguelles, M., Csabai, Z., Datry, T., de Eyto, E., Dohet, A., Dorflinger, G., Drohan, E., Eikland, K. A., England, J., Eriksen, T. E., Evtimova, V., Feio, M. J., Ferreol, M., Floury, M., Forcellini, M., Forio, M. A. E., Fornaroli, R., Friberg, N., Fruget, J. F., Georgieva, G., Goethals, P., Graca, M. A. S., Graf, W., House, A., Huttunen, K. L., Jensen, T. C., Johnson, R. K., Jones, J. I., Kiesel, J., Kuglerova, L., Larranaga, A., Leitner, P., L'Hoste, L., Lizee, M. H., Lorenz, A. W., Maire, A., Arnaiz, J. A. M., McKie, B. G., Millan, A., Monteith, D., Muotka, T., Murphy, J. F., Ozolins, D., Paavola, R., Paril, P., Penas, F. J., Pilotto, F., Polasek, M., Rasmussen, J. J., Rubio, M., Sanchez-Fernandez, D., Sandin, L., Schafer, R. B., Scotti, A., Shen, L. Q., Skuja, A., Stoll, S., Straka, M., Timm, H., Tyufekchieva, V. G., Tziortzis, I., Uzunov, Y., van der Lee, G. H., Vannevel, R., Varadinova, E., Varbiro, G., Velle, G., Verdonschot, P. F. M., Verdonschot, R. C. M., Vidinova, Y., Wiberg-Larsen, P., and Welti, E. A. R.: The recovery of European freshwater biodiversity has come to a halt, Nature, 620, 582-588, https://doi.org/10.1038/s41586-023-06400-1, 2023.

Jackson, F. L., Hannah, D. M., Fryer, R. J., Millar, C. P., and Malcolm, I. A.: Development of spatial regression models for predicting summer river temperatures from landscape characteristics: Implications for land and fisheries management, Hydrol. Processes, 31, 1225-1238, https://doi.org/10.1002/hyp.11087, 2017.

Jacob, D., Petersen, J., Eggert, B., Alias, A., Christensen, O. B., Bouwer, L. M., Braun, A., Colette, A., Déqué, M., Georgievski, G., Georgopoulou, E., Gobiet, A., Menut, L., Nikulin, G., Haensler, A., Hempelmann, N., Jones, C., Keuler, K., Kovats, S., Kröner, N., Kotlarski, S., Kriegsmann, A., Martin, E., van Meijgaard, E., Moseley, C., Pfeifer, S., Preuschmann, S., Radermacher, C., Radtke, K., Rechid, D., Rounsevell, M., Samuelsson, P., Somot, S., Soussana, J.-F., Teichmann, C., Valentini, R., Vautard, R., Weber, B., and Yiou, P.: EURO-CORDEX: new high-resolution climate change projections for European impact research, Regional Environmental Change, 14, 563-578, https://doi.org/10.1007/s10113-013-0499-2, 2013.

https://doi.org/10.5194/egusphere-2025-4550
Preprint. Discussion started: 15 January 2026

Knez, S., Štrbac, S., and Podbregar, I.: Climate change in the Western Balkans and EU Green Deal: status, mitigation and challenges, ENERGY SUSTAIN SOC, 12, https://doi.org/10.1186/s13705-021-00328-y, 2022.

Michel, A., Schaefli, B., Wever, N., Zekollari, H., Lehning, M., and Huwald, H.: Future water temperature of rivers in Switzerland under climate change investigated with physics-based models, Hydrol. Earth Syst. Sci., 26, 1063-1087, https://doi.org/10.5194/hess-26-1063-2022, 2022.

Noyes, P.D. and Lema, S.C.: Forecasting the impacts of chemical pollution and climate change interactions on the health of wildlife, Curr. Zool, 61, 669-689, https://doi.org/10.1093/czoolo/61.4.669, 2015.

Piotrowski, A. P. and Napiorkowski, J. J.: Performance of the air2stream model that relates air and stream water temperatures depends on the calibration method, J HYDROL, 561, 395-412, https://doi.org/10.1016/j.jhydrol.2018.04.016, 2018.

Piotrowski, A. P., Osuch, M., and Napiorkowski, J. J.: Influence of the choice of stream temperature model on the projections of water temperature in rivers, J HYDROL, 601, https://doi.org/10.1016/j.jhydrol.2021.126629, 2021.

Qiu, R., Wang, Y., Rhoads, B., Wang, D., Qiu, W., Tao, Y., and Wu, J.: River water temperature forecasting using a deep learning method, J HYDROL, 595, https://doi.org/10.1016/j.jhydrol.2021.126016, 2021.

Shi, X., Sun, J., and Xiao, Z.: Investigation on River Thermal Regime under Dam Influence by Integrating Remote Sensing and Water Temperature Model, WATER-SUI, 13, https://doi.org/10.3390/w13020133, 2021.

Soomro, S.-e.-h., Shi, X., Guo, J., Ke, S., Hu, C., Asad, M., Jalbani, S., Zwain, H. M., Khan, P., and Boota, M. W.: Are global influences of cascade dams affecting river water temperature and fish ecology?, Appl. Water Sci., 13, https://doi.org/10.1007/s13201-023-01902-9, 2023.

Su, L.: Stable Stream Temperature Prediction for Different Basins Using Time Series Encoding and Temporal Convolutional Networks: TimENC-TCN model, Zenodo [code and data set], https://doi.org/10.5281/zenodo.17185045, 2025 (last access: 23 September 2025).

Sun, J., Di Nunno, F., Sojka, M., Ptak, M., Luo, Y., Xu, R., Xu, J., Luo, Y., Zhu, S., and Granata, F.: Prediction of daily river water temperatures using an optimized model based on NARX networks, Ecol. Indic., 161, https://doi.org/10.1016/j.ecolind.2024.111978, 2024.

Toffolon, M. and Piccolroaz, S.: A hybrid model for river water temperature as a function of air temperature and discharge, Environ. Res. Lett., 10, https://doi.org/10.1088/1748-9326/10/11/114011, 2015.

Tomkins, M., McDonald, H., Huck, J., Tippett, J., Elliot, S., Harris, E. and Maxwell, C.: Modelling the cooling effects of urban canals, 32nd Annual GIS Research UK Conference, Leeds, April 2024, https://doi.org/10.5281/zenodo.10927599

van Vliet, M. T. H., Thorslund, J., Strokal, M., Hofstra, N., Flörke, M., Ehalt Macedo, H., Nkwasa, A., Tang, T., Kaushal, S. S., Kumar, R., van Griensven, A., Bouwman, L., and Mosley, L. M.: Global river water quality under climate change and hydroclimatic extremes, Nat. Rev. Earth Environ., 4, 687-702, https://doi.org/10.1038/s43017-023-00472-3, 2023.

Wade, J., Kelleher, C., and Hannah, D. M.: Machine learning unravels controls on river water temperature regime dynamics, J HYDROL, 623, https://doi.org/10.1016/j.jhydrol.2023.129821, 2023.

https://doi.org/10.5194/egusphere-2025-4550
Preprint. Discussion started: 15 January 2026

Yu, Q., Han, Q., Shi, S., Sun, X., Wang, X., Wang, S., Yang, J., Su, W., Nan, Z., and Li, H.: Metagenomics reveals the response of antibiotic resistance genes to elevated temperature in the Yellow River, Sci Total Environ, 859, 160324, https://doi.org/10.1016/j.scitotenv.2022.160324, 2023.

Zhao, Q., Van den Brink, P. J., Xu, C., Wang, S., Clark, A. T., Karakoc, C., Sugihara, G., Widdicombe, C. E., Atkinson, A., Matsuzaki, S. S., Shinohara, R., He, S., Wang, Y. X. G., and De Laender, F.: Relationships of temperature and biodiversity with stability of natural aquatic food webs, Nat Commun, 14, 3507, https://doi.org/10.1038/s41467-023-38977-6, 2023.

Zhi, W., Klingler, C., Liu, J., and Li, L.: Widespread deoxygenation in warming rivers, Nat. Clim. Change, 13, 1105-1113, https://doi.org/10.1038/s41558-023-01793-3, 2023.

Zhi, W., Ouyang, W., Shen, C., and Li, L.: Temperature outweighs light and flow as the predominant driver of dissolved oxygen in US rivers, Nat. Water, 1, 249-260, https://doi.org/10.1038/s44221-023-00038-z, 2023.

Zhu, S., Di Nunno, F., Sun, J., Sojka, M., Ptak, M., and Granata, F.: An optimized NARX-based model for predicting thermal dynamics and heatwaves in rivers, Sci Total Environ, 926, 171954, https://doi.org/10.1016/j.scitotenv.2024.171954, 2024.

Zhu, S. and Piotrowski, A. P.: River/stream water temperature forecasting using artificial intelligence models: a systematic review, ACTA GEOPHYS, 68, 1433-1442, https://doi.org/10.1007/s11600-020-00480-7, 2020.